Applied Magnetic Resonance
https://doi.org/10.1007/s00723-024-01646-y

Applied
Magnetic Resonance

ORIGINAL PAPER

On the Microstructure and Dynamics of Membranes Formed by Lipid as From *Stenotrophomonas maltophilia*, a Member of Gut Microbiome: An EPR Study

G. Vitiello[1,2] · R. Esposito[2,3] · I. Speciale[3] · C. De Castro[3] · G. D'Errico[2,3]

Received: 17 June 2023 / Revised: 6 December 2023 / Accepted: 1 March 2024

Abstract
Lipid As are the main components of the external leaflet of the outer membrane of Gram-negative bacteria. Their molecular structure has evolved to allow the bacteria survival in specific environments. In the present work, we investigate how and to what extent lipid membranes that include in their composition lipid A molecules of a bacterium of the gut microbiota, *Stenotrophomonas maltophilia*, differ from those formed by the lipid A of the common Gram-negative bacterium *Salmonella enterica*, which is not specific to the gut and is here used as a reference. Electron Paramagnetic Resonance (EPR) spectroscopy, using spin-labelled lipids as molecular probes, allows the segmental order of the acyl chain and the polarity across the bilayer to be analyzed in detail. Both considered lipid As cause a stiffening of the outermost segments of the acyl chains. This effect increases with increasing the lipid A content and is stronger for the lipid A extracted from *Stenotrophomonas maltophilia* than for that extracted from *Salmonella enterica*. At the same time, the local polarity of the bilayer region just below the interface increases. As the inner core of the bilayer is considered, it is found that the lipid A from *Salmonella enterica* causes a local disorder and a significant reduction of the local polarity, an effect not found for the lipid A from *Stenotrophomonas maltophilia*. These results are interpreted in terms of the different lengths and distributions of the acyl tails in the two lipid As. It can be concluded that the symmetrically distributed short tails of the lipid A from *Stenotrophomonas maltophilia* favors a regular packing within the bilayer.

1 Introduction

The domain Bacteria encompasses a large spectrum of prokaryotes, including both beneficial and pathogenic species. While pathogenic bacteria and the molecular determinants of their harmful activity have been extensively investigated throughout the twentieth century, the role played by beneficial ones in the biological context

Extended author information available on the last page of the article

Published online: 11 April 2024

has attracted the deserved attention only in more recent times. Gut microbiota, localized in the human gastrointestinal tract, represents a paramount example of beneficial bacteria, whose biological function includes intestinal epithelium maintenance [1], resistance to pathogens [2], prevention of cancers [3], and redox homeostasis regulation through the gut–brain axis [4]. Most gut bacteria are anaerobes. An important exception is given by the core microbiota found in the crypts of *Lieberkühn* (or intestinal crypts), which is dominated by strictly aerobic, nonfermentative bacteria, including *Acinetobacter, Delftia*, and *Stenotrophomonas* [5]. Considering that bacteria tropism relies on the adaptation of their structure, analysis of specific features presented by these species is of great interest.

Depending on their response to the Gram stain, bacteria are divided into Gram-negative and Gram-positive species (appearing red/pink and dark blue/violet after staining, respectively). The different response derives from the different molecular architecture of the cell wall: in Gram-positive bacteria, the phospholipid bilayer constituting the cytoplasmatic membrane is wrapped by a thick layer of peptidoglycan, a polysaccharide network cross-linked by peptide chains; in Gram-negative bacteria cell wall, the peptidoglycan layer is thinner and is, in turn, wrapped by an asymmetric lipid bilayer named outer membrane. The inner leaflet of the outer membrane is formed by glycerophospholipids, while the external leaflet is composed of lipopolysaccharides (LPS).

LPS are amphiphilic macromolecules comprising a relatively hydrophobic glycolipid, named lipid A, and a long hydrophilic chain, constituted by the core oligosaccharide plus the O-specific polysaccharide or O-chain. Among the LPSs of the various bacterial species, the lipid A portion is the most conserved part, being constituted by an amino sugar disaccharide backbone covalently bonded to an average of six acyl residues [6]. Variations of this primary structure, including the number, distribution, and length of the acyl chains, as well as the eventual phosphorylation and further chemical derivatization of the disaccharide backbone, have been found to tune the lipid A biological activity [7]. In fact, lipid As act as potent stimulators of the innate immune system of mammal hosts, originating a wide range of biological effects, from a significant enhancement of the resistance to bacterial infection, which is beneficial to the host, to an uncontrolled immune response resulting in septic shock [8].

The tight self-assembly of lipid As, which occurs through the combination of hydrophobic and electrostatic interactions, ensures the cell wall integrity and resistance to physical and chemical external agents (as harsh environments or host antimicrobials). Indeed, a lipid A leaflet is more rigid and displays a more ordered structure than a glycerophospholipid layer [9, 10].

LPSs and, more specifically, lipid As of Gram-negative populations in the gut microbiota present chemical peculiarities [11]. In the present work, we investigate how and to what extent lipid membranes formed by lipid As of a crypt-specific bacterium, *Stenotrophomonas maltophilia*, differ from those formed by the lipid A of the common Gram-negative bacterium *Salmonella enterica,* which is not specific to the gut. The molecular structures of the two lipid As are shown in Fig. 1.

We analyze the general attitude of these lipid As to self-aggregate and to aggregate with other lipids, rather than focus on specific biological or bio-mimicking

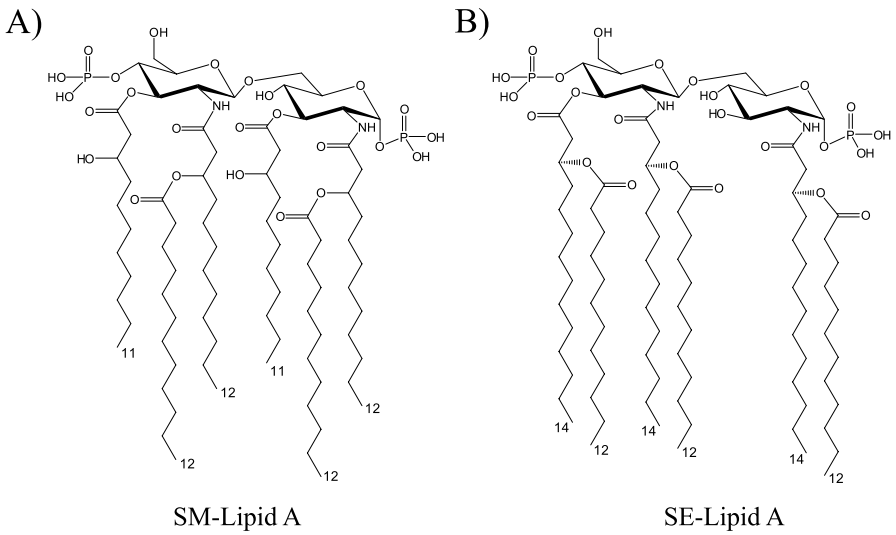

Fig. 1 Molecular structures of the lipid A extracted from *Stenotrophomonas maltophilia* (**A**) and the lipid A extracted from *Salmonella enterica* (**B**)

membranes. For this reason, we considered lipid A mixtures with reference phospholipids whose aggregation behavior is well assessed. The study is performed using simple in vitro models of biomembranes, such as liposomes, investigated by Electron Paramagnetic Resonance (EPR) spectroscopy of spin-labelled lipids as molecular probes. As suggested us by Prof. Carlo Corvaja and his research group in fruitful collaboration works [12, 13], the analysis of the EPR spectral parameters of the nitroxides furnishes a wealth of information on amphiphiles self-assembly. Particularly, starting from 1973, when Schindler and Seelig published their seminal work on the EPR spectra of spin labels in lipid bilayers [14], this technique has proven to be one of the most informative on these systems [15–20]. In this study, we use this approach for a comparative analysis of the structure and dynamics of phospholipid bilayers including one of the two lipid As under investigation.

2 Materials and Methods

2.1 Materials

The lipid A from *Stenotrophomonas maltophilia* (SM-Lipid A) was extracted and purified from murine gut microbiota as reported in a previous work [5] while the lipid A from *Salmonella enterica* serotype minnesota Re 595 (SE-Lipid A) was purchased from Sigma-Aldrich (Milan, Italy). Dichloromethane and methanol, HPLC-grade solvents, were obtained from Merck (Darmstadt, Germany). 1-palmitoyl-2-oleoyl-*sn*-glycero-3-phosphocholine (POPC, 99% purity) and 1-palmitoyl-2-oleoyl-*sn*-glycero-3-phosphoglycerol (POPG, 99% purity) were obtained from Avanti Polar

Lipids (Alabaster, USA). HEPES buffer solution (10 mM), NaCl and $CaCl_2$ salts were obtained from Sigma-Aldrich. Spin-labelled phosphatidylcholines (*n*-PCSL) with the nitroxide group at different positions, $n = 5$, 7, 10 and 14, in the *sn*-2 acyl chain to be used for EPR experiments, were also obtained from Avanti Polar Lipids. The spin-labelled fatty acids (*n*-doxyl stearic acids, *n*-DSA with $n = 5$, 16) were purchased from Sigma-Aldrich. Spin-labels were stored at − 20 °C in ethanol solutions at a concentration of 1 mg/mL.

2.2 Sample Preparation

Large Unilamellar Vesicles (LUVs) of POPC/POPG 70:30 mol:mol, (POPC/POPG):SM-Lipid A and (POPC/POPG):SE-Lipid A at different molar ratios (100:0, 85:15, 70:30, 50:50, 40:60, 20:80 and 0:100) were prepared through lipid films hydration method [21]. For the system (POPC/POPG):SE-Lipid A an additional sample was prepared at 10/90 molar ratio. The lipids were independently dissolved in dichloromethane/methanol mixture (2:1 v/v, 10 mg/mL lipid concentration). Proper volumes of these solutions were used to form lipid mixtures with the above-reported lipid molar ratios and a total lipid amount of 1 mg. At this moment, a proper volume of a stock solution in ethanol (1 mg/mL) of one spin-labelled phosphatidylcholines or fatty acids (*n*-PCSL or *n*-DSA) was also added to the lipid films to have a spin-label content equal to 1%w of the total lipids. The lipid films were produced by evaporating the organic solvents under nitrogen flow. Final traces of the solvents were removed by storing the sample under vacuum for at least 3 h. The lipid films were re-suspended in 1 mL of physiological buffer at pH = 7.2 (150 mM sodium chloride, 10 mM HEPES, 1 mM calcium chloride) and vortexed. The produced Multi Lamellar Vesicles (MLVs) were repeatedly extruded through polycarbonate membranes of 100 nm pore size, for at least 11 times to produce LUV suspensions.

2.3 Electron Paramagnetic Resonance (EPR) spectroscopy

EPR spectra were recorded with a 9 GHz Bruker Elexys E-500 spectrometer (Bruker, Rheinstetten, Germany). The capillaries containing a specific amount (25 µL) of each liposome suspensions were placed in a standard 4 mm quartz sample tube to be measured at 25 °C. The following instrumental settings were used to record the spectra: sweep width, 100 G; resolution, 1024 points; time constant, 20.48 ms; conversion time, 20.48 ms; modulation frequency, 100 kHz; modulation amplitude, 1.0 G; incident power, 6.37 mW. Several scans, typically 32, were collected to improve the signal-to-noise ratio. A quantitative analysis of *n*-PCSL spectra for all considered samples was realized determining the acyl chain order parameter relative to the bilayer normal, *S*, and the isotropic hyperfine coupling constants for the spin-labels in the membrane, a'_N, as defined in the literature [22, 23]. Magnetic field values at which minima and maxima in spectra are observed were determined through a homemade, MATLAB-based software routine, which allows the selection of a limited field range in which the signal is fitted to a gaussian

curve. Uncertainties were determined by repeating each measurement in triplicate on independently prepared samples.

3 Results and Discussion

3.1 Effects of the Lipid A Content on the POPC/POPG Lipid Bilayers Structure

The EPR spectra of the 5-PCSL spin-label included in lipid bilayers of POPC/POPG in the presence of SM-Lipid A at increasing molar ratio are shown in Fig. 2A. Their comparison highlights the effect of the lipid A content on the packing and dynamics of the phospholipid bilayer. Particularly, 5-PCSL bears the reporter nitroxide group close to the hydrophilic lipid headgroup, thus monitoring the region of the bilayer core just underneath the hydrophilic layer formed by the lipid polar heads.

All the spectra show a clearly well-defined axially anisotropic behavior, as detectable by the splitting of the low- and high-field lines, which is typical of this spin labels included in lipid bilayers [24, 25] where the reporter nitroxide group is not free to rotate but assumes a preferential orientation, thus indicating an ordered organization of the outer segments of the lipid acyl chains. The anisotropic degree increases with the content of SM-Lipid A (see the dotted line in Fig. 2), pointing to an enhancement of the lipid ordering within the membrane.

Figure 2B shows the 5-PCSL spectra in (POPC/POPG):SE-Lipid A bilayers. Also for this system the spectrum anisotropy increases with the lipid A content; however, the variation appears lower than that observed in the presence of SM-Lipid A. This is due to the presence of SE-Lipid A which partially hindered the local

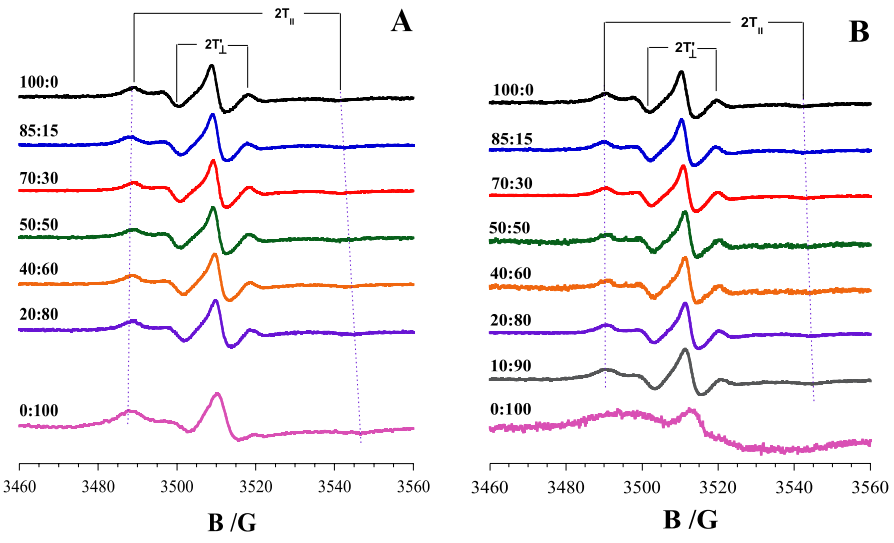

Fig. 2 EPR spectra of 5-PCSL in bilayers of POPC/POPG (70:30 mol:mol) at different content of the lipid A extracted from *Stenotrophomonas maltophilia* (**A**) and *Salmonella enterica* (**B**)

mobility. Interestingly, the 5-PCSL spectrum in the absence of phospholipids, i.e., in SE-Lipid A aqueous mixtures, is broadened by spin–spin interactions between the labelled lipids. This could suggest a tendency of the phospholipid to segregate within the bilayer, thus being not molecularly dispersed. Indeed, perusal of Fig. 2A reveals that some evidence of spin exchange is present even in the sample containing only SM-Lipid A, which however does not preclude a clear detection of the signal of 5-PCSL dispersed in the lipid A bilayer, indicating a better miscibility of phospholipids in SM-Lipid A than in SE-Lipid A. For the system (POPC/POPG):SE-Lipid A an additional measurement was carried out at 10/90 molar ratio.

To gain more quantitative information from the spectra we calculated the order parameter, S, and the isotropic hyperfine coupling constant, a'_N. In particular, S is a measure of the local orientational ordering of the labelled segment of the acyl chain with respect to the normal to the bilayer surface and is calculated according to the relation:

$$S = \frac{(T_{\parallel} + T_{\perp})}{(T_{zz} - T_{\mathrm{xx}})} \frac{a_N}{a'_N} \tag{1}$$

where $T_{\parallel}$ and $T_{\perp}$ are two phenomenological hyperfine splitting parameters that were evaluated from the experimental spectra as shown in Fig. 1 (considering that 2 $T'_{\perp} = 2\ T_{\perp} - 1.6$) [22]. T_{xx} and T_{zz}, which are the main elements of the real hyperfine splitting tensor in the spin Hamiltonian of the spin label, are determinable from the corresponding single-crystal EPR spectrum and are equal to $T_{\mathrm{xx}} = 6.1$ G and $T_{zz} = 32.4$ G, as reported in the literature [26]. a_N and a'_N are the isotropic hyperfine coupling constants for the spin-label in the crystal state and in the membrane, respectively, given by:

$$a_N = \frac{1}{3}(T_{zz} + 2T_{\mathrm{xx}}) \tag{2}$$

$$a'_N = \frac{1}{3}(T_{\parallel} + 2T_{\perp}) \tag{3}$$

a'_N is an index of the micro-polarity experienced by the nitroxide. Analysis of the S and a'_N trends with increasing the lipid A content in the bilayer furnishes detailed information about the changes induced by its presence on the microstructure of phospholipid bilayers.

Inspection of Fig. 3 shows an increase of the order parameter S as increasing amounts of SM-Lipid are included in the bilayer (black squares). This evidence indicates an increase in the local order of the more external part of the bilayer hydrophobic core due to a constrained packing of lipid molecules induced by the presence of SM-Lipid A molecules, which are much bulkier with respect to phospholipids. This effect is rather gradual with changing the bilayer composition; however, it appears more pronounced in the presence of high content of SM-Lipid A. At the same time, an increase in the a'_N values is detected (red squares), indicating an increase of the local polarity experienced by the radical label, suggesting a favoured penetration of the water molecules, at least up to the fifth carbon of the acyl chain, as an effect

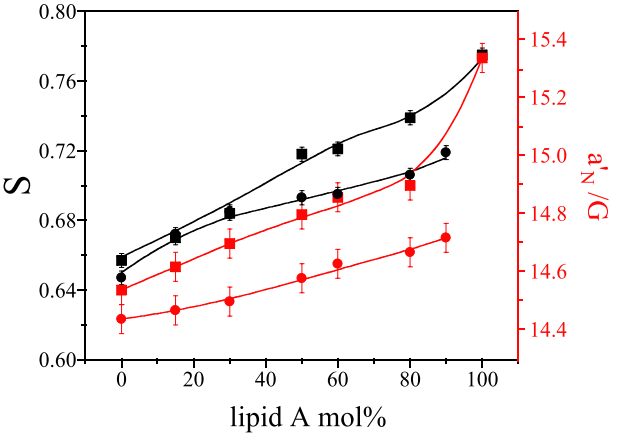

Fig. 3 Trends of the order parameter, *S*, and hyperfine coupling constant, a'_N, determined from EPR spectra of 5-PCSL in the bilayers formed by (POPC/POPG):SM-Lipid A (black and red squares) and (POPC/POPG):SE-Lipid A (black and red circles) of at different lipid A content

of the high hydration of neighbouring lipid A sugar moieties. This phenomenon becomes dramatic for lipid bilayers composed of SM-Lipid A alone.

Figure 3 also shows a significant increase in the *S* value estimated from the 5-PCSL spectra due to the presence of SE-Lipid A (black circles). Up to a content equal to 30 mol % the effect of SE-Lipid A is similar to that detected for SM-Lipid A. However, at higher content, the *S* increase due to the SE-Lipid A is significantly lower than observed for SM-Lipid. For what concerns the coupling constant, a'_N, its increase with the SE-Lipid A content in the bilayer is lower than that observed for SE-Lipid A in the whole investigated lipid A composition range (red circles).

Additional experiments were performed on liposomes formed by the pure SM-Lipid A or SE-Lipid A, as well as by the POPC/POPG mixture, using 5-DSA as a spin-label. Fatty acids seem to be miscible with lipid As, as no evidence of spin-exchange was observed (see Supplementary Information). Analysis of the 5-DSA spectra qualitatively confirmed what was inferred from the 5-PCSL spectra: both lipid As form bilayers in which the region close to the headgroups is more ordered than in phospholipid bilayers, the effect being more evident for SM-Lipid A than for SE-Lipid A.

3.2 Effects of the Lipid A on the POPC/POPG Lipid Bilayer Profile

To further investigate the lipid A effects on the lipid self-assembly and packing within the bilayer, the samples with (POPC/POPG):Lipid A 50:50 mol/mol composition was selected, including either SM-Lipid A or SE-Lipid A. As described in the experimental section, 1 mol % of phosphatidylcholines spin-labelled at the different positions of the s*n*-2 chain (*n*-PCSL, with $n = 5$, 7, 10 or 14) was incorporated in the membrane. Specifically, while 5-PCSL bears the nitroxide reporter group close to the hydrophilic headgroups domain, 7-PCSL and 10-PCSL

are representative of the intermediate segments of the lipid acyl chains while in 14-PCSL the nitroxide group is positioned close to the terminal methyl groups. Therefore, the combined use of different *n*-PCSL spin-labels allowed the entire bilayer profile perpendicular to the membrane surface to be characterized.

The *n*-PCSL spectra in (POPC/POPG):SM-Lipid A 50:50 mol/mol bilayers are shown in Fig. 4, where they are compared to the spectra registered in the absence of lipid A. As discussed above, the 5-PCSL spectra show a well-defined axially anisotropic lineshape. As the reporter nitroxide group is stepped down along the acyl chain from position 5 to 10, the anisotropy markedly decreases. In the case of 14-PCSL, a three-line quasi-isotropic spectrum is observed. This trend, typical of phospholipid membranes in the fluid phase [27], indicates that moving from the bilayer surface to the inner core the ordering of the acyl chain segments progressively decreases as they become freer to rotate and orient in all directions and, consequently, the local fluidity increases. Inspection of Fig. 4 confirms that the fluid state is preserved in the presence of the lipid As in the bilayer composition. Interestingly, in the case of SE-Lipid A, the 10-PCSL spectrum, which shows an anisotropic lineshape in the absence of any lipid A and in the presence of SM-Lipid A, turns to an almost isotropic three-line signal.

Further details of the lipid A effects on the bilayer microstructure are obtained by the quantitative analysis of the experimental spectra. For all investigated systems S shows a decreasing trend with n (Fig. 5A), and becomes very low at position 14, i.e., in the center of the lipid bilayer. a'_N also shows decreasing trends (Fig. 5B), in agreement with the typical condition of lipid membranes whereby the innermost hydrophobic region is characterized by a much lower polarity than the outermost region of the polar heads. Both S and a'_N trends remain qualitatively the same in the presence of SM-Lipid A; however, the lipid A causes

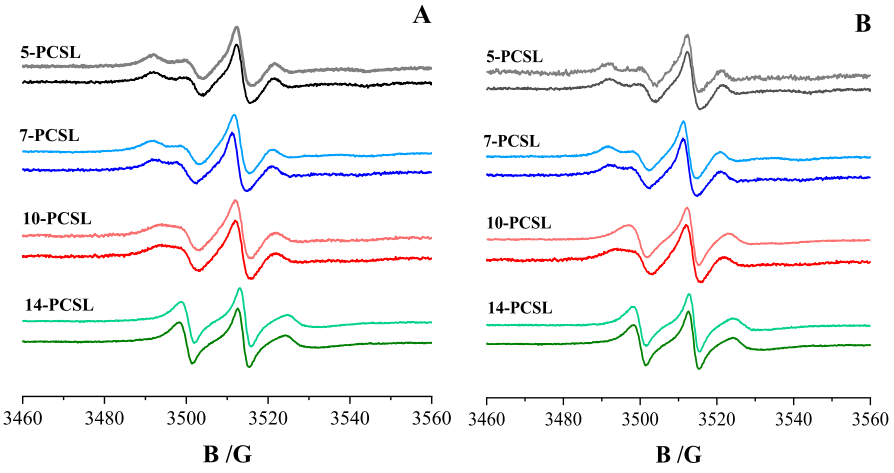

Fig. 4 EPR spectra of *n*-PCSL in bilayers composed of POPC/POPG (dark lines) and (POPC/POPG):Lipid A at 50:50 mol/mol (bright lines). The panels refer to the lipid A extracted from *Stenotrophomonas maltophilia* (**A**) and from *Salmonella enterica* (**B**)

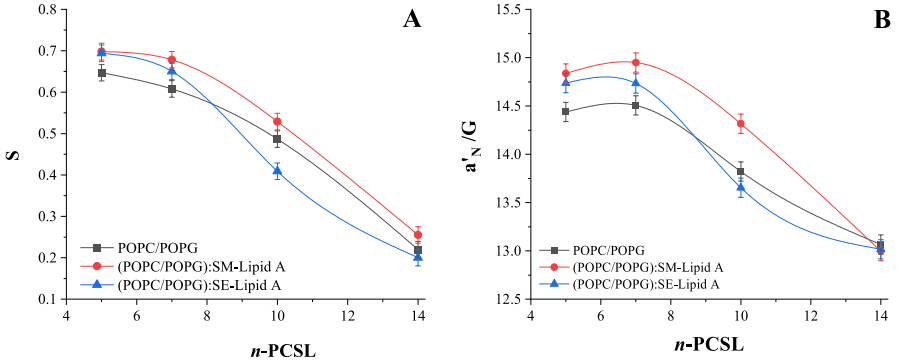

Fig. 5 Trends of (**A**) order parameter, *S*, and (**B**) hyperfine coupling constant, a'_N, determined from the EPR spectra of *n*-PCSL in bilayers composed of POPC:POPG 70:30 mol/mol (black squares), (POPC:POPG)/SM-Lipid A 50:50 mol/mol (red circles) and (POPC:POPG)/SE-Lipid A 50:50 mol/mol (blue triangles)

clearly detectable variations of the observed values. Particularly, the *S* values are higher at all the spin-label positions, the perturbation induced by the presence SM-Lipid A on the lipid bilayer being slightly more pronounced for the outermost region of the bilayer ($\Delta S \approx 0.6$ G for the 5- and 7-PCSL spectra) than for the hydrophobic core ($\Delta S \approx 0.35$ G for 10- and 14-PCSL spectra). Similarly, as shown in Fig. 5B, an increase in the a'_N values was observed for $5 \leq n \leq 10$ while no significant changes was observed in correspondence to the termini of acyl chains, thus confirming that the different steric hindrance due to the SM-Lipid A presence improved the penetration of water molecules in the outer region of the lipid bilayer, an effect not detectable at the center of the inner core.

Interestingly, a different effect is observed when the lipid bilayer containing SE-Lipid A is considered (Fig. 5A). With respect to the POPC/POPG bilayer, the *S* values slightly increase in the outermost region of the bilayer ($\Delta S \approx 0.04$ G for spectra of 5- and 7-PCSL), while an evident *S* decrease is detected for the more internal region ($\Delta S \approx -0.07$ and -0.02 G for spectra of 10- and 14-PCSL, respectively), indicating an increase in the acyl chain freedom to rotate and orient. A similar trend is shown by the a'_N values, thus suggesting that the local disorder of the lipid chain segments more distant from the lipid headgroups disfavors the penetration of water molecules in the inner region of the lipid bilayer.

Additional experiments were performed on liposomes formed by the pure SM-Lipid A or SE-Lipid A, as well as by the POPC/POPG mixture, using 16-DSA as spin-label (see Supplementary Information). Analysis of the 16-DSA spectra qualitatively confirmed that SM-Lipid A form bilayers in which the region close to the acyl chains termini is more ordered than in bilayers formed by SE-Lipid A or by phospholipids.

4 Conclusions

We analysed the effects of two different lipid As on the microstructure of the lipid bilayers in which they are included. SM-Lipid A was extracted from *Stenotrophomonas maltophilia*, a Gram negative bacterium belonging to the gut microbiota. SE-Lipid A was extracted from *Salmonella enterica*, a common and well-studied bacterium chosen as a reference. Our aim is to verify whether the adaptation of the former bacterium to survive in the intestinal crypts is reflected in a peculiar attitude of the lipid A to self-assemble and interact with other lipids.

The results reported and discussed in the previous sections highlighted that both lipid As induce an increase in the rigidity of the more external section of the bilayer; this dose-dependent effect is more marked for SM-Lipid A than for SE-Lipid A. Moreover, a clear difference was observed when the lipid As effect on the properties of the bilayer inner core was analysed: the ordering effect of SM-Lipid A propagates along the whole length of the lipid acyl chains, and only at their termini it becomes negligible; in contrast, SE-Lipid A induces an evident disorder of the inner core. Interestingly, the different local ordering of the acyl chains reflects in a different permeability of the bilayer to water molecules: the disordered and compact packing of lipids in the core of the bilayer containing SE-Lipid A results in a more apolar local environment, thus suggesting a reduced permeability to water molecules, evidence not found for SM-Lipid A.

Our finding could be interpreted based on the molecular structure of lipid As. The steric hinderance of these bulky lipids is expected to induce a rigid organization of the bilayer. However, the different behavior shown by the two examined lipid As highlight that more specific molecular features have to be taken into account. As mentioned in the introduction, lipid As comprise a disaccharide glucosamine backbone phosphorylated at both ends and further substituted with some fatty acids. Regarding the lipid As produced by *Stenotrophomonas maltophilia* and *Salmonella enterica* bacteria, both are hexa-acylated species and they differ in the type of fatty acids and their distribution along the glucosamine disaccharide backbone. In SM-Lipid A, the fatty acids are shorter compared to those of SE, and they are symmetrically distributed being three on each glucosamine unit (Fig. 1). In contrast, in the SE-Lipid A molecular structure, four relatively longer acyl chains are grouped on one glucosamine, only two being bonded to the other one.

It is long known that the length and distribution of lipid A fatty acids impact both the conformation and the activity of these molecules. Indeed, as proposed by the early studies by Seydel et al. [28, 29] the type of fatty acids and their distribution pattern determine the orientation of the glucosamine disaccharide backbone relative to the bacterial membrane surface, namely the level of tilting. The lipid A of *E. coli* or of *Salmonella* species, which are all very similar, have a wide tilt angle, while the symmetrical distribution along with the reduced length of the fatty acids chains is related to a minor tilt angle [30].

It can be proposed that the longer acyl chain, along with the headgroup tilting due to the asymmetrical tail distribution could be responsible for a “higher

crowding" of the bilayer inner core, which leads to a more disordered and compact local molecular organization. At this stage, it is not possible to individuate the direct biological consequences of our finding, but these preliminary data can lay the foundation for further studies directed to assess the relationship between the outer membrane microstructure and the regulation of its function.

Supplementary Information The online version contains supplementary material available at https://doi.org/10.1007/s00723-024-01646-y.

Author Contributions C.D.C. and G.D'E designed the research. I.S. and C.D.C. extracted the lipid A to be used in sample preparation. R.E. and G.V. prepared the samples and performed the electron paramagnetic resonance spectra. G.D'E. and G.V. analyzed the data and wrote the main manuscript text. G.V., R.E. and I.S. prepared the figures. All authors reviewed the manuscript.

Funding Open access funding provided by Università degli Studi di Napoli Federico II within the CRUI-CARE Agreement. No funding was received for this research.

Availability of Data and Materials The data are available upon request to the authors.

Declarations

Conflict of Interest The authors declare that they have no known competing financial interests or personal relationships that could have appeared to influence the work reported in this paper.

Ethical Approval Not applicable.

Consent of Publication We give our consent for the publication of the following manuscript to be published in the Journal–Applied Magnetic Resonance. We understand that this copy may be available in both print and in the Internet, and will be available to a broader audience through marketing channels and other third parties. Therefore, anyone can read material published in the Journal.

References

1. C.M. Arenas-Gómez, E. Garcia-Gutierrez, J.S. Escobar, P.D. Cotter, Crit. Rev. Microbiol. (2022). https://doi.org/10.1080/1040841X.2022.2142088
2. L. Xu, C.S. Yang, Y. Liu, X. Zhang, Front. Pharmacol. (2022). https://doi.org/10.3389/fphar.2022.895193
3. D. Beyoglu, J.R. Idle, Biochem. Pharmacol. (2022). https://doi.org/10.1016/j.bcp.2022.115225
4. Y. Wang, Z. Zhang, B. Li, B. He, L. Li, E.C. Nice, W. Zhang, J. Xu, Antioxidants (2022). https://doi.org/10.3390/antiox11112287
5. T. Naito, C. Mulet, C. De Castro, A. Molinaro, A. Saffarian, G. Nigro, M. Bérard, M. Clerc, A.B. Pedersen, P.J. Sansonetti, T. Pédron, MBio (2017). https://doi.org/10.1128/mBio.01680-17

6. A. Molinaro, O. Holst, F. Di Lorenzo, M. Callaghan, A. Nurisso, G. D'Errico, A. Zamyatina, F. Peri, R. Berisio, R. Jerala, J. Jiménez-Barbero, A. Silipo, S. Martín-Santamaría, Chem. Eur. J. (2015). https://doi.org/10.1002/chem.201403923
7. M.A. Valvano, Microbiology (2022). https://doi.org/10.1099/mic.0.001159
8. P. Garcia-Vello, F. Di Lorenzo, D. Zucchetta, A. Zamyatina, C. De Castro, A. Molinaro, Pharmacol. Ther. (2022). https://doi.org/10.1016/j.pharmthera.2021.107970
9. G. D'Errico, A. Silipo, G. Mangiapia, G. Vitiello, A. Radulescu, A. Molinaro, R. Lanzetta, L. Paduano, Phys. Chem. Chem. Phys. (2010). https://doi.org/10.1039/c0cp00066c
10. G. D'Errico, A. Silipo, G. Mangiapia, A. Molinaro, L. Paduano, R. Lanzetta, Phys. Chem. Chem. Phys. (2009). https://doi.org/10.1039/b816248d
11. F. Di Lorenzo, C. De Castro, A. Silipo, A. Molinaro, FEMS Microbiol. Rev. (2019). https://doi.org/10.1093/femsre/fuz002
12. G.A.A. Saracino, A. Tedeschi, G. D'Errico, R. Improta, L. Franco, M. Ruzzi, C. Corvaja, V. Barone, J. Phys. Chem. A (2002). https://doi.org/10.1021/jp026492e
13. A.M. Tedeschi, L. Franco, M. Ruzzi, L. Paduano, C. Corvaja, G. D'Errico, Phys. Chem. Chem. Phys. (2003). https://doi.org/10.1039/b305324p
14. H. Schindler, J. Seelig, J. Chem. Phys. (1973). https://doi.org/10.1063/1.1680269
15. D. Marsh, Proc. Natl. Acad. Sci. U.S.A. (2001). https://doi.org/10.1073/pnas.131023798
16. W.K. Subczynski, J. Widomska, J.B. Feix, Free Radic. Biol. Med. (2009). https://doi.org/10.1016/j.freeradbiomed.2008.11.024
17. P. Stepien, A. Polit, A. Wisniewska-Becker, Biochim. Biophys. Acta (2015). https://doi.org/10.1016/j.bbamem.2014.10.004
18. R. Guzzi, R. Bartucci, Arch. Biochem. Biophys. (2015). https://doi.org/10.1016/j.abb.2015.06.015
19. E. Laudadio, R. Galeazzi, G. Mobbili, C. Minnelli, A. Barbon, M. Bortolus, P. Stipa, ACS Omega (2019). https://doi.org/10.1021/acsomega.8b03395
20. M. Schmallegger, A. Barbon, M. Bortolus, A. Chemelli, I. Bilkis, G. Gescheidt, L. Weiner, Langmuir (2020). https://doi.org/10.1021/acs.langmuir.0c01585
21. H. Zhang, Methods Mol. Biol. (2017). https://doi.org/10.1007/978-1-4939-6591-5_2
22. W. Hubbell, H.M. McConnell, J. Am. Chem. Soc. (1971). https://doi.org/10.1021/ja00731a005
23. A. Luchini, D. Cavasso, A. Radulescu, G. D'Errico, L. Paduano, G. Vitiello, Langmuir (2021). https://doi.org/10.1021/acs.langmuir.1c00981
24. A. Lange, D. Marsh, K.H. Wassmer, P. Meier, G. Kothe, Biochemistry (1985). https://doi.org/10.1021/bi00337a020
25. A. Falanga, R. Tarallo, G. Vitiello, M. Vitiello, E. Perillo, M. Cantisani, G. D'Errico, M. Galdiero, S. Galdiero, PLoS ONE (2012). https://doi.org/10.1371/journal.pone.0032186
26. L.M. Gordon, R.D. Sauerheber, Biochim. Biophys. Acta (1977). https://doi.org/10.1016/0005-2736(77)90206-1
27. G. D'Errico, A.M. D'Ursi, D. Marsh, Biochemistry (2008). https://doi.org/10.1021/bi7025062
28. U. Seydel, M. Oikawa, K. Fukase, S. Kusumoto, K. Brandenburg, Eur. J. Biochem. (2000). https://doi.org/10.1046/j.1432-1033.2000.01326.x
29. S. Roes, U. Seydel, T. Gutsmann, Langmuir (2005). https://doi.org/10.1021/la048218c
30. S.M. Zughaier, H.C. Ryley, S.K. Jackson, Infect. Immun. (1999). https://doi.org/10.1128/iai.67.3.1505-1507.1999

Authors and Affiliations

G. Vitiello[1,2] · R. Esposito[2,3] · I. Speciale[3] · C. De Castro[3] · G. D'Errico[2,3]

✉ G. Vitiello
giuseppe.vitiello@unina.it

✉ G. D'Errico
gerardino.derrico@unina.it

[1] Department of Chemical, Materials and Production Engineering, University of Naples Federico II, Piazzale Tecchio 80, 80125 Naples, Italy

[2] CSGI, Center for Colloid and Surface Science, via della Lastruccia 3, 50019 Sesto Fiorentino (FI), Italy

[3] Department of Chemical Science, University of Naples Federico II, Complesso di Monte Sant'Angelo, via Cinthia 4, 80126 Naples, Italy